

Structural Investigation of Asymmetrical Dimer Radical Cation System (H₂O–H₂S)⁺: Proton-Transferred or Hemi-Bonded?

Ravi Joshi,[†] Tapan K. Ghanty,^{*,‡} Sergej Naumov,[§] and Tulsi Mukherjee^{||}

Radiation and Photochemistry Division, and Theoretical Chemistry Section, and Chemistry Group, Bhabha Atomic Research Center, Mumbai 400 085, India, and Leibniz Institute of Surface Modification, Permoserstrasse 15, 04303 Leipzig, Germany

Received: November 22, 2006

Ab initio molecular orbital and hybrid density functional methods have been employed to characterize the structure and bonding of (H₂O–H₂S)⁺, an asymmetrical dimer radical cation system. A comparison has been made between the two-center three-electron (2c-3e) hemi-bonded system and the proton-transferred hydrogen-bonded systems of (H₂O–H₂S)⁺. Geometry optimization of these systems was carried out using unrestricted Hartree Fock (HF), density functional theory with different functionals, and second-order Møller–Plesset perturbation (MP2) methods with 6-311++G(d,p) basis set. Hessian calculations have been done at the same level to check the nature of the equilibrium geometry. Energy data were further improved by calculating basis set superposition error for the structures optimized through MP2/6-311++G(d,p) calculations. The calculated results show that the dimer radical cation structure with H₂O as proton acceptor is more stable than those structures in which H₂O acts as a proton donor or the 2c-3e hemi-bonded (H₂O··SH₂)⁺ system. This stability trend has been further confirmed by more accurate G3, G3B3, and CCSD(T) methods. On the basis of the present calculated results, the structure of H₄O⁺ can best be described as a hydrogen-bonded complex of H₃O⁺ and SH with H₂O as a proton acceptor. It is in contrast to the structure of neutral (H₂O··H₂S) dimer where H₂O acts as a proton donor. The present work has been able to resolve the ambiguity in the nature of bonding between H₂O and H₂S in (H₂O–H₂S)⁺ asymmetrical dimer radical cation.

1. Introduction

Structural investigation of hydrogen-bonded complexes is of great theoretical and experimental interest due to their importance in many chemical and biological systems and processes.¹ The strength of a hydrogen bond depends on the proton donating and proton accepting ability of the donor and the acceptor, respectively. Sometimes, the type of interaction involved in the hydrogen bond is also controversial.² The asymmetrical dimer system (H₂O–H₂S) is an interesting example in this context. H₂O has good proton donating as well as accepting ability whereas H₂S is neither a good proton donor nor a good proton acceptor. There are various reports on the detailed theoretical investigation of neutral asymmetrical dimer system (H₂O–H₂S) suggesting an almost linear intermolecular hydrogen bond between H₂O and H₂S.^{3–7} However, the results obtained from different studies are not mutually consistent. For example, in some studies H₂O has been found to act as a proton donor,^{3,4} whereas in others it has been found to act as a proton acceptor.^{5–7} In recent years, hydrogen-bonded systems with an excess proton (H⁺ ion) or OH[–] ion have attracted considerable attention^{8–17} both from experimentalists and theoreticians due to their fundamental importance and anomalous behavior. Among these species H₅O₂⁺ and H₃O₂[–] are the two prototype examples, which have been investigated extensively. Both these

species can be obtained through addition/removal of a proton to/from the hydrogen-bonded neutral water dimer system. However, comparatively less attention has been devoted to the ionized hydrogen-bonded systems obtained through removal/addition of an electron from/to the neutral system. It is to be noted that ionized hydrogen-bonded systems exhibit a very rich and varied chemistry. The ionized hydrogen-bonded systems can evolve via different chemical reactions such as electron transfer, proton transfer, or molecular rearrangement.

Among various ionized hydrogen-bonded systems, dimer radical cation/anion species have fascinated researchers because of their ambiguous structures. These dimer radical cation (H₂X)₂⁺ or anion (H₂X)₂[–] species are formed by intermolecular interaction between a neutral molecule and molecular cation or anion, respectively. Here, X is an atom from first or second row of periodic table. It has been shown that generally hydrogen-bonded systems are preferred for all the first-row systems whereas 2c-3e hemi-bond is preferred for the second-row systems. However, both kind of systems have similar energies for (H₃P)₂⁺ species.¹⁸ For second-row (H₂X)₂⁺ systems, unpaired electron in the p-orbital of heteroatom gets stabilized by coordination with a free p-electron pair on another neutral heteroatom, making a 2c-3e hemi-bond which is not the case with the first row dimer radical cations. For example, proton transferred structure (H₃O⁺··OH) is known to be favored for (H₂O)₂⁺ system,^{18–21} but the 2c-3e hemi-bonded structure (H₂S··SH₂)⁺ is known to be preferred for the (H₂S)₂⁺ system.^{18,21–23}

In the present study, the asymmetrical dimer radical cation system (H₂O–H₂S)⁺ has been selected, which has hetero atoms (oxygen and sulfur) of both first and second row each.

* To whom correspondence should be addressed. E-mail: tapang@barc.gov.in.

[†] Radiation and Photochemistry Division, Bhabha Atomic Research Center.

[‡] Theoretical Chemistry Section, Bhabha Atomic Research Center.

[§] Leibniz Institute of Surface Modification.

^{||} Chemistry Group, Bhabha Atomic Research Center.

CHART 1: Structures of (H₂O–H₂S)⁺ System

(HO ^{••+} SH ₃)	(HS ^{••+} OH ₃)	(H ₂ O [•] :SH ₂) ⁺
I	II	III
H ₂ O as proton donor	H ₂ O as proton acceptor	Hemi-bonded system

Ionization-induced changes in the structure and nature of bonding of such asymmetrical dimer (H₂O–H₂S) are of interest, which is in between the dimer radical cation systems (H₂O)₂⁺ and (H₂S)₂⁺. However, the (H₂O–H₂S)⁺ system has not been studied in detail. Moreover, there are contradictory reports in the literature on the structure of (H₂O–H₂S)⁺ system. Clark has reported that (H₂O–H₂S)⁺ has hemi-bonded structure in C_s symmetry.²³ On the other hand, a later study suggested against a hemi-bonded structure for (H₂O–H₂S)⁺ system²⁴ based on the absence of any orbital overlapping. Consequently, proton transferred structure may be considered as another alternative for (H₂O–H₂S)⁺. However, there is no systematic report on the proton transferred or hydrogen-bonded structure of (H₂O–H₂S)⁺. Moreover, this system (H₄OS⁺) might be considered in between the protonated and the deprotonated species mentioned above, and may serve as a prototype example of the ionized hydrogen-bonded systems involving hetero atoms. Therefore, three different possible structures have been considered for geometry optimization of (H₂O–H₂S)⁺ (see Chart 1): (1) structure I, H₂O can act as proton donor (PD) producing (HO^{••+}SH₃); (2) structure II, H₂O can act as proton acceptor (PA) producing (H₃O⁺••SH); or (3) structure III, a 2c-3e hemi-bonded (H₂O[•]:SH₂)⁺. Among these, structures I and II seem to be more probable because water can act both as a proton acceptor and a proton donor.

In the ab initio calculations of such dimer radical cation/anion system the importance of electron correlation and need for larger basis set is well-known.²¹ Further, symmetry restrictions are known to affect the optimization of such species. Therefore, it is also interesting to compare the stability of the hemi-bonded structure with the proton-transferred structures of (H₂O–H₂S)⁺ using correlated methods with large basis sets.

It is to be noted that selection of different methods and functional leads to different structure and energy in the theoretical calculations of (H₂O)₂⁺.^{18–21,25–27} The calculations based on post-HF, DFT with 50% exact HF exchange (BHHLYP functional), and modified coupled pair functional (MCP) methods have predicted proton-transferred (HO^{••+}OH₃) structure to be a minimum.^{18,20} On the other hand, DFT with a few gradient-corrected functionals (such as BLYP, B3LYP, etc.) has predicted hemi-bonded as the minimum-energy structure.^{25–27} However, both DFT and post-HF calculations for (H₂S)₂⁺ lead to the same result predicting hemi-bonded structure as the lower-energy isomer, although the energy difference between the proton transferred and the hemi-bonded structure varies from one method to another.^{18,21–23} These studies indicate that DFT-predicted results depend on the selection of functionals. Therefore, it is interesting to compare the results for (H₂O[•]:SH₂)⁺ system obtained using different functionals as well as different computational methods.

To the best of our knowledge, thorough study of various possible structures of this system and their comparison has not been performed. In the present study, pure density functional method has not been used since it fails to predict the correct structure of weakly bonded dimer radical species. Pure density functional method also fails to predict the relative stability of different structures as compared to post-HF based methods. Thus, in this work our objective is to find the global minimum structure of (H₂O–H₂S)⁺ system using density functional

method with various hybrid functionals and also by MP2 method. The MP2 optimized structures have been further investigated using G3, G3B3 and CCSD(T) methods to improve the results obtained by DFT and MP2 methods.

2. Computational Methods

The three different possible structures I–III (shown in Chart 1) have been used for (H₂O–H₂S)⁺ system. The proton-transferred structures (I and II) have been compared with hemi-bonded structure III. Ab initio molecular orbital methods have been used to get the energy of the optimized (H₂O–H₂S)⁺ system and its possible constituents H₂O, H₂S, H₂O⁺, H₂S⁺, H₃O⁺, H₃S⁺, OH, and SH. Unrestricted Hartree–Fock (HF), density functional theory with B3LYP, BHHLYP and HLYP functionals, and second-order Møller–Plesset perturbation (MP2) methods have been used for the geometry optimization. The ab initio calculations have been performed using the GAMESS²⁸ electronic structure program with 6-311++G(d,p) basis set for hydrogen, oxygen, and sulfur atoms. Stable structures were characterized using vibrational analysis. Binding energy (BE) has been calculated by subtracting the total energy of the structure from the total energy of the constituent species.

Quantum chemical calculations for structures I–III have been also performed with Gaussian03²⁹ program using G3 and G3B3 methods.³⁰ G3 theory (Gaussian-3) is one of the most accurate methods for calculating energies of molecules containing atoms of the first and second row of the periodic table. G3 theory uses geometries from second-order perturbation theory [MP2-(FU)/6-31G(d)] and scaled zero-point energies from Hartree–Fock theory [HF/6-31G(d)] followed by a series of single-point energy calculations at MP2 level, fourth-order Møller–Plesset (MP4), and quadratic configuration interaction [QCISD(T)] levels of theory. The MP4 calculations are carried out with the 6-31G(d) basis set and several basis set extensions. The QCISD(T) calculation is done with the 6-31G(d) basis set. The MP2 calculation is performed with a new basis set, referred to as G3 large, and includes core correlation. The other single-point energy calculations are done with a frozen core approximation. G3 theory is effectively at the QCISD(T,FU)/G3 large level and makes certain assumptions about additivity of the calculations. It also includes a spin–orbit correction, and a higher-level correction. G3B3 method is a variant of G3 method and uses the B3LYP density functional method for geometries and zero-point energies in place of the MP2/6-31G(d) geometries and scaled HF/6-31G(d) zero-point energies, respectively. The G3B3 results are known to be slightly improved compared to G3 for inorganic hydrides and radicals.³⁰ Further, G3 energy is expected to be more precise than G3B3 energy for asymmetrical (H₂O–H₂S)⁺ system due to the use of density functional in G3B3 method. To further ascertain the stability order of the three structures, their geometries and energies have been calculated using more accurate CCSD/cc-pVTZ method followed by single point energy calculation using CCSD(T)/aug-cc-pVTZ level of theory.

3. Results and Discussion

DFT and MP2 Calculations. Three possible structures for (H₂O–H₂S)⁺ systems (Chart 1) have been considered to investigate the structure, energy, and nature of bonding of this system. The stability of the proton-transferred systems has also been compared with the hemi-bonded system. The geometries of structures I–III have been fully optimized without any symmetry restriction using HF, DFT with different functionals, and MP2 methods. The structures optimized with MP2 method

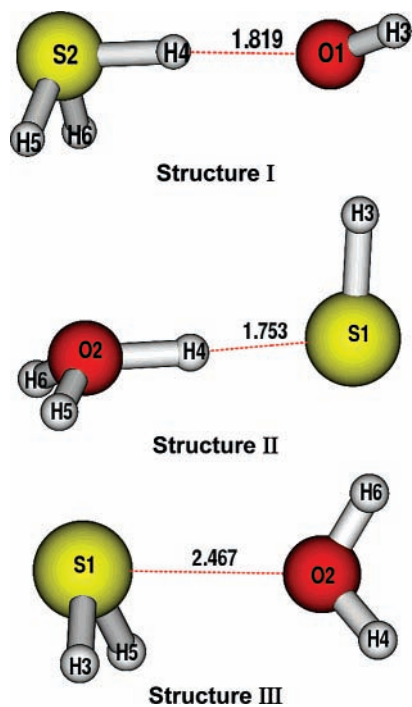


Figure 1. Optimized geometrical structures of $(\text{H}_2\text{O}-\text{H}_2\text{S})^+$ by MP2 method.

are shown in Figure 1. The bond lengths and bond orders for all the structures are given in Table 1. Structure II with H_2O as PA and H_2S as PD has been found to be more stable as compared to the hemi-bonded structure III and proton transferred structure I (H_2O as PD) by HF, DFT with different functionals, and MP2 method. Total energy of structures I–III follows an order I (-474.732813 au) > III (-474.791081 au) > II (-474.794045 au) as calculated by MP2 method. However, it is in contrast to the structure of neutral $(\text{H}_2\text{O}-\text{H}_2\text{S})$ system where H_2O acts as a proton donor. In an earlier study, another asymmetrical system $(\text{H}_2\text{O}:\cdot\text{NH}_3)^+$ has not been found to have a hemi-bonded structure as the global minimum.²⁰ Further, Clark has also reported that the strongest 2c-3e hemi-bond is expected between the fragments of similar ionization potentials only.²³ The calculation of ionization potential of H_2O and H_2S in the present study has also suggested that it is easier to ionize H_2S than H_2O . Since ionization of the species increases its acidity, H_2S^+ should donate a proton to H_2O to produce $(\text{H}_3\text{O}^+\cdots\text{SH})$, i.e., structure II. Considering the better spin localization on larger sulfur atom as compared to that on oxygen atom, this is quite expected.

The energy of structures I and III with respect to structure II is given in Table 2. Table 2 also lists the zero-point energy corrected relative energies of the structures I and III with respect to structure II as calculated using different methods. It has been observed that both HF and DFT methods underestimate the energy difference for structure I. However, for structure III there is no regular trend in the relative energies. To understand the distribution of unpaired electron on asymmetrical dimer radical cation $(\text{H}_2\text{O}-\text{H}_2\text{S})^+$ system, Mulliken atomic spin population, free valence, and Mulliken charges have been calculated (Table 3) for the structures optimized by MP2 method. The bond lengths between the two fragments of $(\text{H}_2\text{O}-\text{H}_2\text{S})^+$ (both hydrogen-bonded and hemi-bonded) as calculated using different methods are shown in Table 4. The length of the weakest bond between the two fragments for structures I, II, and III has been calculated to be 1.819, 1.753, and 2.467 Å, respectively, by MP2 method. For structure I, the O(1)–H(4) bond (1.819 Å)

has become almost double of O(1)–H(3) bond (0.973 Å for H_2O). The corresponding bond order is reduced by ~ 7 times. Bond order of O(1)–H(4) has been calculated to be 0.126, whereas for all other bonds it is ≥ 0.8 for structure I. This suggests that proton (H4) is transferred from H_2O to H_2S and the fragments H_3S^+ and OH are held together by hydrogen bond in structure I (Figure 1). The calculated Mulliken atomic spin population (reported in Table 3) is also the highest on the oxygen atom (O(1)), thereby suggesting the formation of OH in agreement with the structure $\text{H}_3\text{S}^+\cdots\text{OH}$.

Similarly for structure II the S(1)–H(4) bond (1.753 Å) of H_2S has been stretched to 1.3 times of S(1)–H(3) bond (1.343 Å), and the corresponding bond order is reduced. S(1)–H(4) bond order (0.750) for structure II has been calculated to be ~ 6 times as compared to O(1)–H(4) of structure I (0.126). Also, the bond order of O(2)–H(4) for structure II (0.446) has been calculated to be nearly half of that of S(2)–H(4) for structure I (0.819). This suggests that the extent of proton transfer is more in structure I as compared to that in structure II. In other words, the most stable structure (II) has a partial proton transfer from H_2S to H_2O as compared to that for structure I. The calculated Mulliken atomic spin population is highest on the sulfur atom for structure II (S(1)), suggesting the formation of SH is in agreement with the structure $\text{H}_3\text{O}^+\cdots\text{SH}$. The results indicate that there is a proton transfer from H_2S to H_2O in structure II, and the fragments H_3O^+ and SH are held together through a hydrogen bond. Dihedral angle $\angle 6241$ for the structures I and II are 27.52° and 115.96° , respectively. The bond angle $\angle 413$ for structures I and II are 142.26° and 96.21° , respectively.

The optimized structure III has been associated with a larger distance (2.467 Å) between S(1) of H_2S and O(2) of H_2O , suggesting against a bond between H_2S and H_2O . This value is also close to the average (~ 2.4 Å) of the hemi bond in $(\text{H}_2\text{O})_2^+$ and $(\text{H}_2\text{S})_2^+$ reported earlier.^{18,21,24} Even the corresponding bond order is calculated to be low enough (0.086) to make a bond between H_2S and H_2O . All other bonds for structure III have bond order values > 0.8 . The calculated spin density is highest on S(1) atom, indicating ionization of the constituent of lower ionization potential, H_2S . Total energy, bond length, and bond order values calculated for structure III agree well with those reported earlier.^{23,24}

A small bond order (0.086) and large bond length (2.467 Å) between the constituents of structure III suggest that the 2c-3e hemi-bond is weak enough to exist. Bond lengths and bond orders for the structures I and II indicate that they have proton-transferred hydrogen-bonded system. The bond length (1.753 Å) and bond order (0.750) values of the most stable structure (II) suggest a partially proton-transferred hydrogen-bonded system for $(\text{H}_2\text{O}-\text{H}_2\text{S})^+$. The study suggests that ionization produces a drastic change in the geometry of $(\text{H}_2\text{O}-\text{H}_2\text{S})$ dimer system. This is clearly evident from the structures of the neutral dimer (H_2O as proton donor)³ as compared to the ionized dimer (H_2O as proton acceptor). It is to be noted that ionization changes the structure from hydrogen-bonded to proton-transferred hydrogen-bonded structure for $(\text{H}_2\text{O})_2$, whereas the structure changes from hydrogen-bonded to hemi-bonded structure for $(\text{H}_2\text{S})_2$.^{18–22,24,27,31}

A comparison of relative energies calculated for the three different structures (Table 2) shows structure II as the most stable one followed by structures III and I. Zero-point-energy-corrected energy values also follow the same order of stability: II (H_2O as PA) > III (hemi-bonded) > I. (H_2O as PD). This trend agrees well with the presumption that the fragment of lower ionization potential (H_2S) should ionize first and the

TABLE 1: Optimized Geometrical Parameters of (H₂O–H₂S)⁺ by MP2 Method

structure I (HO ^{•••} +SH ₃)		structure II (HS ^{•••} +OH ₃)		structure III (H ₂ O : SH ₂) ⁺	
bond length (Å)	bond order	bond length (Å)	bond order	bond length (Å)	bond order
O(1)–H(3) = 0.973	O(1)–H(3) = 0.872	O(2)–H(4) = 1.129	O(2)–H(4) = 0.446	O(2)–H(4) = 0.965	O(2)–H(4) = 0.856
O(1)–H(4) = 1.819	O(1)–H(4) = 0.126	O(2)–H(5) = 0.971	O(2)–H(5) = 0.835	O(2)–H(6) = 0.965	O(2)–H(6) = 0.863
S(2)–H(5) = 1.345	S(2)–H(5) = 0.913	O(2)–H(6) = 0.971	O(2)–H(6) = 0.835	S(1)–H(3) = 1.344	S(1)–H(3) = 0.914
S(2)–H(6) = 1.345	S(2)–H(6) = 0.916	S(1)–H(3) = 1.343	S(1)–H(3) = 0.930	S(1)–H(5) = 1.344	S(1)–H(5) = 0.914
S(2)–H(4) = 1.369	S(2)–H(4) = 0.819	S(1)–H(4) = 1.753	S(1)–H(4) = 0.750	S(1)–O(2) = 2.467	S(1)–O(2) = 0.086

TABLE 2: Relative Energy (ΔE, kcal/mol) of Various Optimized Geometrical Structures of (H₂O–H₂S)⁺ with Respect to Structure II (HS^{•••}+OH₃)

method	structure I (HO ^{•••} +SH ₃)		structure III H ₂ O : SH ₂) ⁺	
	ΔE	ΔE _{ZPE} ^a	ΔE	ΔE _{ZPE} ^a
HF	23.8	20.0	4.4	2.8
B3LYP	35.5	32.9	0.3	0.7
BHLLYP	32.7	29.8	3.0	2.8
HLYP	28.9	25.6	4.5	3.5
MP2	38.4	36.8	1.9	2.3

^a Zero-point energy corrected relative energy.**TABLE 3: Binding Energy (BE, kcal/mol)^a and Other Parameters of Various Structures of (H₂O–H₂S)⁺**

	structure I (HO ^{•••} +SH ₃)	structure II (HS ^{•••} +OH ₃)	structure III (H ₂ O : SH ₂) ⁺
maximum spin density	O(1) (1.04)	S(1) (1.13)	S(1) (1.01)
maximum free valence charge	O(1) (1.22)	S(1) (1.25)	S(1) (1.13)
	O(1) –0.24	O(2) –0.22	O(2) –0.59
	S(2) +0.35	S(1) +0.33	S(1) +0.55
BE (HF)	11.3	15.9	18.2
BE (B3LYP)	13.8	23.1	26.6
BE (BHLLYP)	13.4	21.0	23.5
BE (HLYP)	14.0	19.7	23.0
BE (MP2)	12.8	22.7	21.0
BE (MP2) _{BSSE} ^b	11.6	20.2	19.0

^a The constituents considered are HO and ⁺SH₃ for structure I, HS and ⁺OH₃ for structure II and H₂O and H₂S⁺ for structure III. ^bBasis set superposition error corrected binding energy.**TABLE 4: Distance (Å) between the Fragments for Various Structures of (H₂O–H₂S)⁺**

method	structure I (HO ^{•••} +SH ₃)	structure II (HS ^{•••} +OH ₃)	structure III (H ₂ O : SH ₂) ⁺
HF	1.966	2.055	2.610
B3LYP	1.729	1.811	2.464
BHLLYP	1.790	1.885	2.426
HLYP	1.826	1.947	2.441
MP2	1.819	1.753	2.467
G3	1.785	1.933	2.389
CCSD	1.826	1.903	2.418

increased acidity of H₂S⁺ results in transfer of a proton to H₂O. This is also in agreement with the better stabilization of spin (unpaired electron) on fragment with more diffuse 3p orbitals of the sulfur atom. It must be noted that the relative energy of (H₂O–H₂S)⁺ system calculated by B3LYP method is closest to that obtained by MP2 method (Table 2). Further, the energy of structure III (hemi-bonded) is a little more (1.9 kcal/mol), but that of structure I (H₂O as PD) is very high (38.4 kcal/mol) as compared to that of structure II (H₂O as PA). This suggests that for the asymmetrical dimer radical cation system, the proton-transferred structure with transfer of proton from the fragment of lower ionization potential is the most stable one.

The calculated Mulliken atomic spin population and free valence have been found to be highest (≥1.0) on O(1), S(1), and S(1) for structures I, II, and III, respectively. Mulliken charge on oxygen atom for structures I, II, and III are calculated to be –0.24, –0.22, and –0.59, respectively. Similarly, Mul-

liken charges on sulfur atom for structures I, II and III are calculated to be 0.35, 0.33, and 0.55, respectively. These values suggest that there is more charge separation in hemi-bonded structure III as compared to that in proton-transferred structures I and II. There is a large difference of Mulliken charges on atoms H(3) (0.31) and H(4) (0.17) of proton donor H₂O, but it is the same (~0.2) on atoms H(5) and H(6) of proton acceptor H₂S for structure I. Similarly, Mulliken charge on atoms H(3), H(4), H(5), and H(6) is 0.11, 0.05, 0.36, and 0.36, respectively, for structure II. However, Mulliken charges on hydrogen atoms of H₂O and H₂S for hemi-bonded structure III are ~0.33 and ~0.17, respectively.

On the basis of Mulliken atomic spin populations, Mulliken charge and free valence values of the optimized structures, it has been considered that constituents of structure I are OH and ⁺SH₃ and those for structure II are SH and ⁺OH₃. Since Mulliken atomic spin population is highest on S(1) of H₂S for structure III, it is assumed that constituents of structure III are H₂O and H₂S⁺. Binding energies of structures I–III have also been calculated with respect to their above-mentioned constituents using HF, DFT with different functionals, and MP2 methods. A comparison of binding energies of the structures I–III (Table 3) shows that the stability of these structures against dissociation into the assumed fragments is high and follows the order II (22.7 kcal/mol) > III (21.0 kcal/mol) > I (12.8 kcal/mol). It is interesting to note that the binding energy of the structures I–III follows the same trend as that of the total energy.

It has been often argued that binding energy of weakly bonded system is overestimated due to basis set superposition error (BSSE).^{32,33} BSSE arises due to the fact that finite size basis sets are used and the basis set on one unit lowers the calculated energy of the other unit at the nuclear configurations of the two subsystems at equilibrium geometry and vice versa. To avoid this problem, BSSE has been estimated for the structures optimized by MP2 method (Table 3). The BSSE corrected interaction energy (ΔE_{BSSE}) values have been found to be very close to the corresponding uncorrected values and also follow the same order, i.e., II (20.2 kcal/mol) > III (19.0 kcal/mol) > I (11.6 kcal/mol). ΔE_{BSSE} values have been calculated to be lower by ≤2.5 kcal/mol only as compared to their corresponding uncorrected values by MP2 method. BSSE corrected energies also suggest that structure II (H₂O as PA) is the most stable structure on ionization of (H₂O–H₂S) dimer.

The calculated bond length connecting the two fragments of (H₂O–H₂S)⁺ are given in Table 4. The MP2 calculated distance between the two fragments for these structures follows the order III (2.47 Å) > I (1.82 Å) > II (1.75 Å). It has been observed that HF overestimates the weak bond (length) between the two constituents in the hydrogen-bonded structures I–II as well as in the hemi-bonded structure III. The weak bond (O(1)–H(4)) in structure I has been calculated to be 1.73–1.83, ~1.97, and ~1.82 Å by DFT with different functional and HF and MP2 methods, respectively. Similarly, the weak bond (S(1)–H(4)) in structure II has been calculated to be 1.81–1.95, ~2.05, and ~1.75 Å by DFT with different functional and HF and MP2

TABLE 5: Energy Values (au) of Structures I, II, and III as Calculated by G3, G3B3, and CCSD(T) Methods

method	structure I (HO \cdots +SH $_3$)	structure II (HS \cdots +OH $_3$)	structure III (H $_2$ O \cdots :SH $_2$) $^+$
G3	-475.211965	-475.264451	-475.262787
G3 (0 K)	-475.217884	-475.269659	-475.267616
G3B3	-475.214983	-475.269395	-475.264004
G3B3 (0 K)	-475.220148	-475.274244	-475.268991
CCSD(T)/cc-pVTZ	-474.872607	-474.932381	-474.925127
CCSD(T)/aug-cc-pVTZ	-474.883250	-474.941546	-474.936183

methods, respectively. Hemi-bond distance in structure III has been calculated to be close to 2.6 Å by HF and 2.4 Å by DFT with different functionals and MP2 method. Earlier, hemi-bonded and proton-transferred structures of symmetrical dimer radical cations (H $_2$ O) $_2^+$ and (H $_2$ S) $_2^+$ have been studied using various methods and functionals.²¹ The average value of the hemi-bonds for (H $_2$ O) $_2^+$ and (H $_2$ S) $_2^+$ structures, as calculated earlier by different methods, is close to that calculated for (H $_2$ O–H $_2$ S) $^+$ in the present work. But the average value of the proton transferred hydrogen bond for (H $_2$ O) $_2^+$ and (H $_2$ S) $_2^+$ structures, as calculated earlier by different methods, is 3–8% more than that calculated for structure II and $\pm(1-3)\%$ for structure I.

G3, G3B3 and CCSD(T) Calculations. In the present work, geometry optimization and energy calculation of an asymmetrical dimer radical cation system involving a weak interaction has been studied using DFT with different hybrid functionals and MP2 methods. However, DFT as well as MP2 methods have been subjected to criticism for the investigations of asymmetrical cation radical systems.^{34–36} Further, the most stable structure II is only 2.3 kcal/mol lower in energy than the hemi-bonded structure III as predicted by MP2 method. In view of this, the structures and energetics of (H $_2$ O–H $_2$ S) $^+$ is further studied with advanced methods of calculation. The G3 procedure is renowned for predicting accurate energy and energy differences for such systems.³⁷ Therefore, (H $_2$ O–H $_2$ S) $^+$ has also been studied using G3, G3B3, and CCSD(T) methods. It is to be noted that the length of the weakest bond between the two fragments for structures I, II, and III has been calculated to be 1.785, 1.933, and 2.389 Å, respectively, by the G3 method (reported in Table 4). The corresponding values using the CCSD method (reported in the same Table) are found to be 1.826, 1.903, and 2.418 Å for the structures I, II, and III, respectively. Thus, the length of the weakest bond is found to be almost the same for structure I; however, for structure II the corresponding MP2 calculated value is the smallest one among all the predicted values reported here. For structure III, the MP2-calculated weakest bond length is found to be close to the corresponding B3LYP predicted value. Therefore, no regular trend has been found as far as different computational methods are concerned for the prediction of the weakest bond length in the three different structures of (H $_2$ O–H $_2$ S) $^+$ system.

The calculated energy trend (Table 5) for structures I–III using G3 and G3B3 methods supports the result of MP2 calculations. Structure II has been calculated to be the most stable, with an energy difference of 1.0 and 3.4 kcal/mol in comparison to structure III, as calculated by G3 and G3B3 methods, respectively. The energy of these structures as calculated by G3 and G3B3 method follows the order I > III > II (Table 5). CCSD(T) calculations have also been performed for the structures I, II and III (Table 5). The CCSD(T) calculated energy values also show that stability of these structures follow the order II > III > I. Structure II has been calculated to be the most stable one with 4.5 and 3.4 kcal/mol more stable than

TABLE 6: Vibrational (IR) Frequencies (cm $^{-1}$) with Intensities (km/mol) for the Three Structures as Calculated by B3LYP Method

structure I		structure II		structure III	
frequencies	intensity	frequencies	intensity	frequencies	intensity
110.9	209.2	127.7	76.8	147.1	79.5
208.9	58.7	287.8	143.8	264.5	12.6
278.7	7.8	409.5	107.3	386.7	6.2
324.8	41.9	522.1	193.7	427.1	41.8
456.6	110.6	573.6	8.0	536.3	88.9
1068.0	15.0	1028.1	105.6	588.2	78.3
1214.0	2.7	1358.9	2737.3	1187.0	0.6
1242.7	5.9	1511.5	37.0	1606.4	63.7
2068.3	1481.5	1752.3	1560.9	2619.0	38.2
2614.6	43.1	2621.4	12.7	2633.4	42.3
2623.2	56.8	3682.7	161.7	3702.6	311.3
3652.0	120.2	3777.9	312.9	3804.2	180.8

structure III, as calculated by CCSD/cc-pVTZ and CCSD(T)/aug-cc-pVTZ methods, respectively (Table 5).

Vibrational frequencies as calculated by DFT-B3LYP method for the three structures are given in Table 6. These calculated IR frequencies suggest that the three structures should have absorption at different positions, which need experimental investigation. Though 2c-3e hemi-bond has been considered between H $_2$ O and H $_2$ S for structure III initially, its geometry optimization has produced H $_2$ O and H $_2$ S $^+$ as two separate fragments. In a recent study, however, the onset of symmetry breaking in 2c-3e symmetrical dimer radical cation for (H $_2$ O) $_2^+$ and (H $_2$ S) $_2^+$ structures has been found at 2.14 and 3.38 Å between the two fragments.³⁶ This suggests that symmetry breaking in asymmetrical dimer radical cation takes place at shorter distances as compared to that in symmetrical radical cation.

4. Concluding Remarks

Ab initio calculations using HF, DFT with different functionals, and MP2, G3, G3B3, and CCSD(T) methods have been performed to characterize the structure and bonding of (H $_2$ O–H $_2$ S) $^+$, an asymmetrical dimer radical cation system. A comparison has been made between the two-center three-electron (2c-3e) hemi-bonded system and the proton-transferred hydrogen-bonded systems of (H $_2$ O–H $_2$ S) $^+$. The dimer radical cation structure with H $_2$ O as proton acceptor is found to be more stable than those structures in which H $_2$ O acts as a proton donor or the 2c-3e hemi-bonded (H $_2$ O \cdots :SH $_2$) $^+$ system. This stability trend has been predicted through DFT with hybrid functionals, MP2, G3, G3B3, and CCSD(T) methods. On the basis of the present calculated results, the structure of H $_4$ OS $^+$ can best be described as a hydrogen-bonded complex of H $_3$ O $^+$ and SH with high Mulliken atomic spin on sulfur atom. It is in contrast to the structure of neutral (H $_2$ O \cdots :H $_2$ S) dimer, where H $_2$ O acts as a proton donor. The present study suggests that on ionization there is a partial proton transfer from the constituent of lower ionization potential to the other one in the case of (H $_2$ X–YH $_2$) $^+$ system. The present work has been able to resolve the ambiguity in the nature of bonding between H $_2$ O and H $_2$ S in (H $_2$ O–H $_2$ S) $^+$ asymmetrical dimer radical cation.

Acknowledgment. We thank Dr. S. K. Ghosh and Dr. S. K. Sarkar for the encouragement during the course of this work.

References and Notes

- (1) Jeffrey, G. A.; Saenger, W. *Hydrogen Bonding in Biological Structures*; Springer: Berlin, 1991. Jeffrey, G. A. *An Introduction to Hydrogen Bonding*; Oxford University Press: New York, 1997.

- (2) Ghanty, T. K.; Staroverov, V. N.; Koren, P. R.; Davidson, E. R. *J. Am. Chem. Soc.* **2000**, *122*, 1210.
- (3) Wang, Y. B.; Tao, F. M.; Pan, Y. K. *Chem. Phys. Lett.* **1994**, *230*, 480.
- (4) Kollman, P.; McKlevey, J.; Johanssen, A.; Rothenberg, S. *J. Am. Chem. Soc.* **1975**, *97*, 955.
- (5) Chin, S.; Ford, T. A. *J. Mol. Struct. (THEOCHEM)* **1985**, *133*, 193.
- (6) Amos, R. D. *Chem. Phys.* **1986**, *104*, 145.
- (7) DelBene, J. E. *J. Phys. Chem.* **1988**, *92*, 2874.
- (8) Robertson, W. H.; Diken, E. G.; Price, E. A.; Shin, J. W.; Johnson, M. A. *Science* **2003**, *299*, 1367.
- (9) Asmis, K. R.; Pivonka, N. L.; Santambrogio, G.; Brummer, M.; Kaposta, C.; Neumark, D. M.; Woste, L. *Science* **2003**, *299*, 1375.
- (10) Headrick, J. M.; Diken, E. G.; Walters, R. S.; Hammer, N. I.; Christie, R. A.; Cui, J.; Myshakin, E. M.; Duncan, M. A.; Johnson, M. A.; Jordon, K. D. *Science* **2005**, *308*, 1765.
- (11) Asthagiri, D.; Pratt, L. R.; Kress, J. D.; Gomez, M. A. *Proc. Natl. Acad. Sci. U.S.A.* **2004**, *101*, 7229.
- (12) Tachikawa, M.; Shiga, M. *J. Am. Chem. Soc.* **2005**, *127*, 11908.
- (13) Huang, X.; Braams, B. J.; Carter, S.; Bowman, J. M. *J. Am. Chem. Soc.* **2004**, *126*, 5042.
- (14) Ludwig, R. *Angew. Chem., Int. Ed.* **2003**, *42*, 258.
- (15) Marx, D.; Tuckermann, M. E.; Hutter, J.; Parrinello, M. *Nature* **1999**, *397*, 601.
- (16) Tuckermann, M. E.; Marx, D.; Hutter, J.; Parrinello, M. *Nature* **2002**, *417*, 925.
- (17) Mohammed, O. F.; Pines, D.; Dreyer, J.; Pines, E.; Nibbering, E. T. *J. Science* **2005**, *310*, 83.
- (18) Gill, P. M. W.; Radom, L. *J. Am. Chem. Soc.* **1988**, *110*, 4931.
- (19) Novalovskaya, Y. V.; Stepanov, N. F. *J. Phys. Chem.* **1999**, *103*, 3285.
- (20) Sodupe, M.; Oliva, A.; Bertran, J. *J. Am. Chem. Soc.* **1994**, *116*, 8249.
- (21) Ghanty, T. K.; Ghosh, S. K. *J. Phys. Chem. A* **2002**, *106*, 11815.
- (22) Sodupe, M.; Oliva, A.; Bertran, J. *J. Am. Chem. Soc.* **1995**, *117*, 8416.
- (23) Clark, T. *J. Am. Chem. Soc.* **1988**, *110*, 1672.
- (24) Maity, D. K. *J. Phys. Chem. A* **2002**, *106*, 5716 and references therein.
- (25) Ghanty, T. K.; Ghosh, S. K.; *J. Phys. Chem. A* **2002**, *106*, 4200.
- (26) Barnett, R. N.; Landman, U. *J. Phys. Chem. A* **1997**, *101*, 164.
- (27) Sodupe, M.; Bertran, J.; Santiago, L. R.; Baerends, E. J. *J. Phys. Chem. A* **1999**, *103*, 166.
- (28) Schmidt, M. W.; Baldrige, K. K.; Boatz, J. A.; Elbert, S. T.; Gordon, M. S.; Jensen, J. H.; Koseki, S.; Matsunaga, N.; Nguyen, K. A.; Su, S. J.; Windus, T. L.; Dupuis, M.; Montgomery, J. A., Jr. *J. Comput. Chem.* **1993**, *14*, 1347.
- (29) Frisch, M. J.; Trucks, G. W.; Schlegel, H. B.; Scuseria, G. E.; Robb, M. A.; Cheeseman, J. R.; Zakrzewski, V. G.; Montgomery, J. A., Jr.; Stratmann, R. E.; Burant, J. C.; Dapprich, S.; Millam, J. M.; Daniels, A. D.; Kudin, K. N.; Strain, M. C.; Farkas, O.; Tomasi, J.; Barone, V.; Cossi, M.; Cammi, R.; Mennucci, B.; Pomelli, C.; Adamo, C.; Clifford, S.; Ochterski, J.; Petersson, G. A.; Ayala, P. Y.; Cui, Q.; Morokuma, K.; Malick, D. K.; Rabuck, A. D.; Raghavachari, K.; Foresman, J. B.; Cioslowski, J.; Ortiz, J. V.; Baboul, A. G.; Stefanov, B. B.; Liu, G.; Liashenko, A.; Piskorz, P.; Komaromi, I.; Gomperts, R.; Martin, R. L.; Fox, D. J.; Keith, T.; Al-Laham, M. A.; Peng, C. Y.; Nanayakkara, A.; Challacombe, M.; Gill, P. M. W.; Johnson, B.; Chen, W.; Wong, M. W.; Andres, J. L.; Gonzalez, C.; Head-Gordon, M.; Replogle, E. S.; Pople, J. A. *GAUSSIAN 03*, Revision B.02: Gaussian, Inc.: Pittsburgh PA, 2003.
- (30) Baboul, A. G.; Curtiss, L. A.; Redfern, P. C. *J. Chem. Phys.* **1999**, *110*, 7650.
- (31) Tsujii, H.; Takizawa, K.; Koda, S. *Chem. Phys.* **2002**, *285*, 319.
- (32) Clementi, E. *J. Chem. Phys.* **1967**, *46*, 3851.
- (33) Xantheas, S. S. *J. Chem. Phys.* **1996**, *104*, 8821.
- (34) Braid, B.; Hiberty, P. C.; Savin, A. *J. Phys. Chem. A* **1998**, *102*, 7872.
- (35) Braid, B.; Hiberty, P. C. *J. Phys. Chem. A* **2000**, *104*, 4618.
- (36) Braid, B.; Lauvergnat, D.; Hiberty, P. C. *J. Chem. Phys.* **2001**, *115*, 90.
- (37) Curtiss, L. A.; Raghavachari, K.; Redfern, P. C.; Rassolov, V.; Pople, J. A. *J. Chem. Phys.* **1998**, *109*, 7764.